

CHAPTER VIII

BIS(2-PHENYLAZOPYRIDINE)(TRIAZENE 1-OXIDATO)

RUTHENIUM(II) PERCHLORATE MONOHYDRATE

## CHAPTER VIII

### BIS(2-PHENYLAZOPYRIDINE)(TRIAZENE 1-OXIDATO)RUTHENIUM(II) PERCHLORATE MONOHYDRATE

Abstract: Tris bidentate heterochelates of type  $[\text{Ru}(\text{pap})_2\text{T}]\text{ClO}_4 \cdot \text{H}_2\text{O}$  analogous to  $[\text{Ru}(\text{bpy})_2\text{T}]\text{ClO}_4 \cdot \text{H}_2\text{O}$  (Chapter VII) obtained by the reaction of substituted triazene 1-oxides ( $\text{R}=\text{Et}$ ;  $\text{X}=\text{OMe}, \text{Me}, \text{H}, \text{Cl}, \text{CO}_2\text{Et}, \text{NO}_2$ ) with bis(2-phenylazopyridine)ruthenium(II) moiety are described. The complexes have  $\text{RuN}_5\text{O}$  coordination environment. These are uniformly 1:1 electrolyte in acetonitrile solution and are diamagnetic ( $t_2^6$ ). In the visible region they exhibit two MLCT bands ( $\sim 720 \text{ nm}$  and  $\sim 550 \text{ nm}$ ).

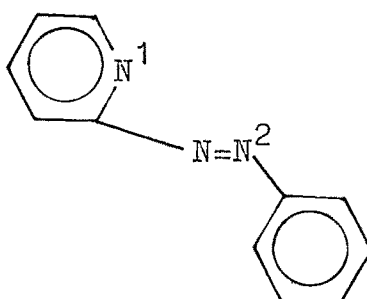
An one-electron nearly reversible ( $\Delta E_p = \sim 70 \text{ mV}$  at  $v \ll 50 \text{ mVs}^{-1}$ ) couple ruthenium(III) +  $e^- \rightleftharpoons$  ruthenium(II) is observed for all complexes in acetonitrile solution ( $E_{298}^0$  lies in the range: 0.71 to 0.93V vs SCE). The  $E_{298}^0 - \sigma$  plot is satisfactorily linear ( $\rho = 0.19\text{V}$ ).

The complexes display ligand reduction responses at the azo function of the pap moiety (-0.4 to -2.3V vs SCE). The  $E_{298}^0$  values of the couples at  $\sim -0.5V$  and  $\sim -1.0V$  shift with substituents present at the triazene 1-oxide frame. A fair to good linear Hammett correlations are observed ( $\rho = 0.09V$ , couple  $\sim -0.5V$ ;  $\rho = 0.13V$ , couple  $\sim -1.0V$ ).

The coulometrically oxidized species  $[\text{Ru}(\text{pap})_2\text{T}]^{2+}$  exhibit, in the visible region, three bands at  $\sim 740$  nm,  $\sim 550$  nm and  $\sim 500$  nm. The lowest energy band is assigned to  $\pi(\text{T}) \rightarrow t_2(\text{Ru})$  and other two bands due to  $\pi(\text{pap}) \rightarrow t_2(\text{Ru})$  (LMCT).

VIII.1 INTRODUCTION

Ruthenium gives rise to interesting azopyridine complexes<sup>1,2</sup>. The ligand 2-(phenylazo)pyridine (I)



I

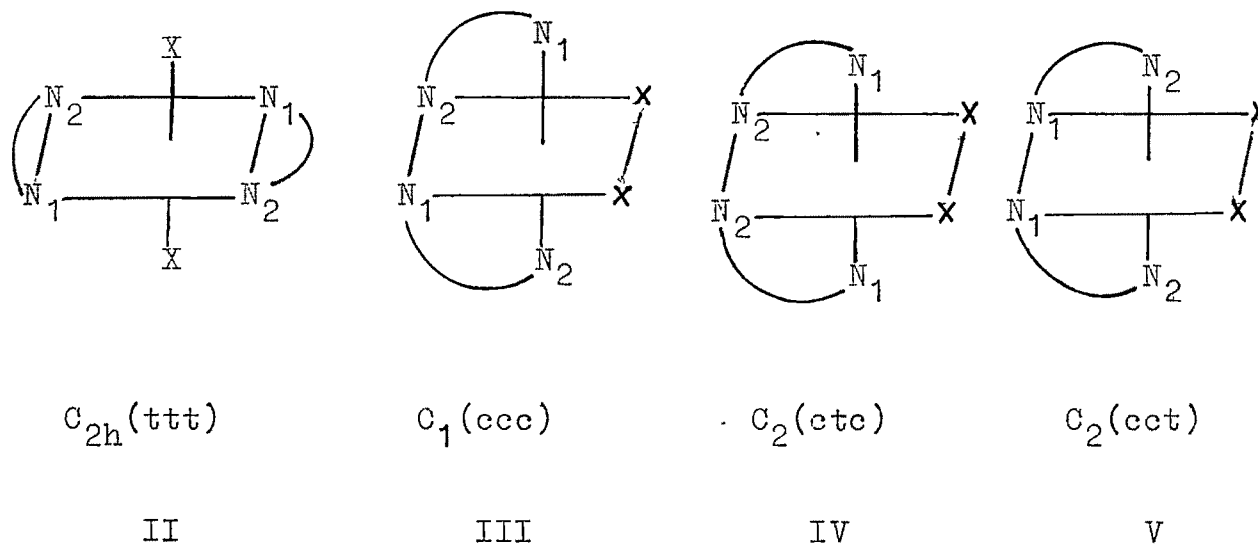
abbreviated as pap is a stronger  $\pi$ -acceptor than 2,2'-bipyridine (bpy).

In this chapter, the binding of triazene 1-oxides to the  $\text{Ru}(\text{pap})_2^{2+}$  moiety is described. The synthesis, characterization and electron transfer properties of complexes of type  $[\text{Ru}(\text{pap})_2\text{T}]\text{ClO}_4 \cdot \text{H}_2\text{O}$  are reported.

VIII.2 RESULTS AND DISCUSSIONA. Synthesis and Structure

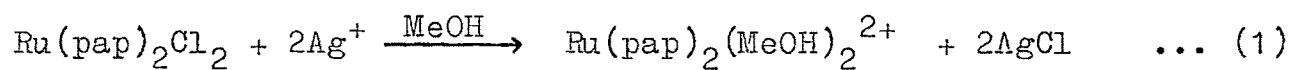
The dihalospecies  $\text{Ru}(\text{pap})_2\text{X}_2$  have thus far been obtained in three isomeric forms<sup>1,2</sup>, one of which is green and other two are blue.

Considering the coordinated atoms in three pairs viz., X,X; N<sub>1</sub>,N<sub>1</sub> and N<sub>2</sub>,N<sub>2</sub>, the green isomer has trans-trans-trans (ttt) configuration, II and one of the blue isomers has cis-cis-cis (ccc) structure, III. On refluxing in xylene, both ttt and ccc isomers are converted to the C<sub>2</sub> isomer: ctc, IV or cct, V.



Recently preliminary crystal structure analysis<sup>3</sup> of the C<sub>2</sub>-Ru(pap)<sub>2</sub>Cl<sub>2</sub> has shown that halogen and azonitrogen (N<sub>2</sub>) are in trans configuration. Hence, the C<sub>2</sub> form is ctc(IV) and not cct(V).

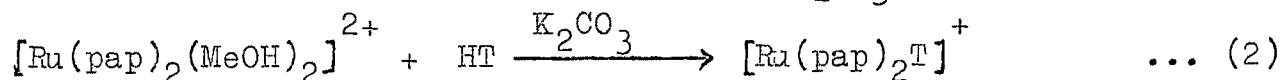
Nucleophilic halide displacement<sup>1</sup> from IV by AgClO<sub>4</sub> in dry methanol at reflux temperature produces violet coloured [Ru(pap)<sub>2</sub>(MeOH)<sub>2</sub>]<sup>2+</sup>.



IV

The disolvento species was then refluxed under nitrogen atmosphere

with one equivalent of HT in presence of  $K_2CO_3$  for 2h.

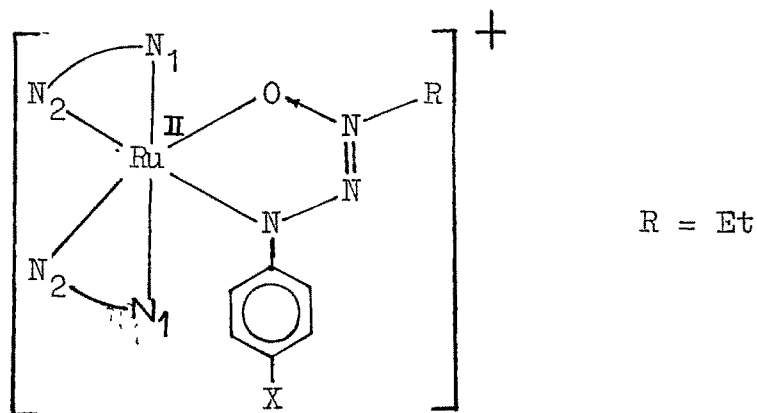


On concentrating the reaction mixture and addition of aqueous  $NaClO_4$  resulted isolation of crystalline red-violet complexes,  $[Ru(pap)_2T]ClO_4 \cdot H_2O$ .

It is to be noted here that the synthesis is carried out at refluxing methanol but the product did not get contaminated with any  $\{RuNO\}^{3+}$  species (compare with Chapter VII). Thus, pap stabilises ruthenium(II) better than bpy.

The complexes are uniformly diamagnetic ( $t_2^6$ ) and behave as 1:1 electrolyte<sup>4</sup> in acetonitrile (Table VIII.1). These are soluble in polar solvents like  $CH_3OH$ ,  $C_2H_5OH$ ,  $CH_3CN$  and insoluble in  $C_6H_6$  and  $(C_2H_5)_2O$ .

Since they are derived from IV, the complexes probably have the structure VI. The complexes are designated by the serial



VI

numbers: X = OMe, 1; Me, 2; H, 3; Cl, 4;  $CO_2Et$ , 5;  $NO_2$ , 6.

Table VIII.1

Solution Molar Electrical Conductivity ( $\Lambda_M$ , mho  $\text{cm}^2\text{mol}^{-1}$ )  
of  $[\text{Ru}(\text{pap})_2\text{T}]\text{ClO}_4 \cdot \text{H}_2\text{O}$  Complexes in Acetonitrile at 298K

| Complex  | $10^3 \times$ Concentration<br>(M) | $\Lambda_M$ |
|----------|------------------------------------|-------------|
| <u>1</u> | 1.02                               | 128         |
| <u>2</u> | 0.77                               | 136         |
| <u>3</u> | 1.19                               | 142         |
| <u>4</u> | 0.84                               | 126         |
| <u>5</u> | 0.84                               | 118         |
| <u>6</u> | 0.90                               | 132         |

## B. Infrared Spectra

The infrared spectra of all complexes (1-6) display characteristic vibrations for coordinated 2-(phenylazo)pyridine<sup>1,2</sup> and triazene 1-oxide<sup>5</sup>. Selected data are given in Table VIII.2 and Fig. VIII.1.

## C. Electronic Spectra

The results obtained on examining the UV-VIS spectra of the complexes are collected in Table VIII.3 and representative spectra are displayed in Fig. VIII.2.

In the visible region, two bands appear at  $\sim 720$  nm and  $\sim 550$  nm. The former absorption is of relatively low intensity. We believe this is due to  $t_2(\text{Ru}) \rightarrow \pi^*(\text{T})(\text{MLCT})$  transition. The band at  $\sim 550$  nm is assigned to  $t_2(\text{Ru}) \rightarrow \pi^*(\text{pap})(\text{MLCT})$  transition as is observed<sup>2</sup> for cis- $\text{Ru}(\text{pap})_2\text{X}_2$  species.

## D. Redox Activity

### (a) The Ruthenium(III)-Ruthenium(II) Couple

The electrochemical activity of all the complexes (1-6) were studied using cyclic voltammetry (CV) at platinum working electrode. All complexes display well defined anodic ( $E_{\text{pa}}$ ) and cathodic ( $E_{\text{pc}}$ ) peaks in acetonitrile (0.1M in TEAP, 298K) in the positive side of SCE (0.71 to 0.93V). Electrochemical data at 298K are collected in Table VIII.4 and representative CVgrams are displayed in Fig. VIII.3.



Table VIII.2

Selected Infrared Frequencies<sup>a, b</sup> ( $\text{cm}^{-1}$ ) of  $[\text{Ru}(\text{pap})_2\text{TlClO}_4 \cdot \text{H}_2\text{O}]$  Complexes

| Complex               | $\nu_{\text{H}_2\text{O}}$ | $\delta_{\text{H}_2\text{O}}$ | $\nu_{\text{C}\cdots\text{O}}$ + $\nu_{\text{C}=\text{N}}$ | $\nu_{\text{N}\rightarrow\text{O}}$ | $\nu_{\text{ClO}_4^-}$ |
|-----------------------|----------------------------|-------------------------------|--|-------------------------------------|------------------------|
| <u>1</u>              | 3420                       | 1620                          | 1590   | 1240                                | 1085, 615              |
| <u>2</u>              | 3420                       | 1620                          | 1590   | 1235                                | 1080, 610              |
| <u>3</u>              | 3420                       | 1620                          | 1590   | 1240                                | 1080, 615              |
| <u>4</u>              | 3420                       | 1620                          | 1590   | 1240                                | 1080, 615              |
| <u>5</u> <sup>c</sup> | 3440                       | 1620                          | 1590   | 1270                                | 1080, 605              |
| <u>6</u>              | 3420                       | 1620                          | 1575   | 1280                                | 1085, 605              |

<sup>a</sup> Measurements were done in KBr disc (4000-250  $\text{cm}^{-1}$ ). <sup>b</sup>  $\nu_{\text{H}_2\text{O}}$ , broad and strong;  $\delta_{\text{H}_2\text{O}}$ , broad and weak;  $\nu_{\text{C}\cdots\text{O}}$  +  $\nu_{\text{C}=\text{N}}$ , sharp and strong;  $\nu_{\text{N}\rightarrow\text{O}}$ , broad and strong;  $\nu_{\text{ClO}_4^-}$ ,  $\sim 1100 \text{ cm}^{-1}$  is broad and very strong,  $\sim 610 \text{ cm}^{-1}$  is sharp and strong. <sup>c</sup>  $\nu_{\text{C}=\text{O}}$  at 1700  $\text{cm}^{-1}$ , broad and strong.

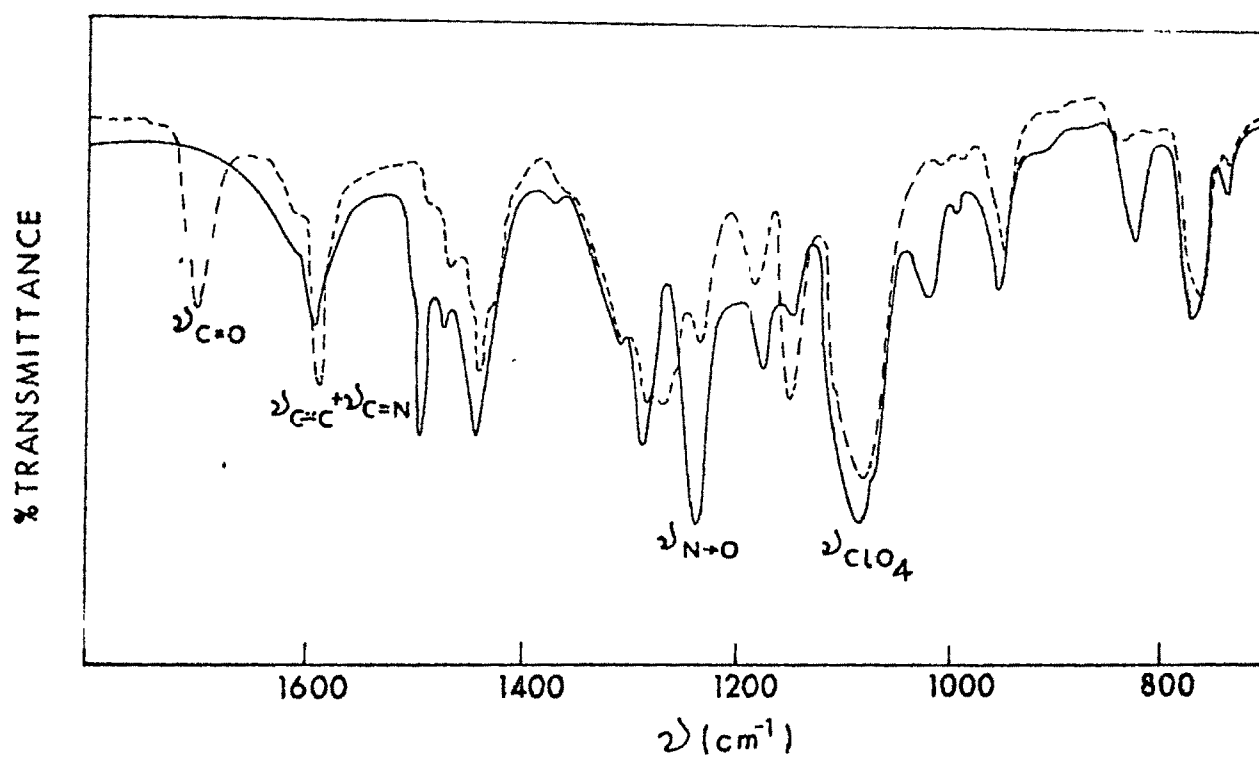


FIG. VIII. 1. INFRARED SPECTRA OF 1 (—) AND 5 (---) IN KBr DISC

Table VIII.3

Electronic Spectral Data of  $[\text{Ru}(\text{pap})_2\text{TlClO}_4 \cdot \text{H}_2\text{O}]$  Complexes in Acetonitrile Solution

| Complex  | $\lambda_{\text{nm}}, (\epsilon, \text{M}^{-1} \text{cm}^{-1})$ |   |
|----------|---|---|
|          | MLCT bands  | Other bands   |
| <u>1</u> | 710(2100), 552(7000)  | 348sh(19700), 318(21700), 216(30400)                  |
| <u>2</u> | 728(1900), 552(7600)  | 360sh(18700), 318(22700), 216(27900)                  |
| <u>3</u> | 730sh(1500), 550(6700)  | 364sh(16400), 318(21900), 218(28600)                  |
| <u>4</u> | 714(1900), 550(7400)  | 360sh(18700), 316(22500), 218(29800)                  |
| <u>5</u> | 716(2200), 548(7600)  | 362sh(20700), 320(22900), 272sh(18000),<br>216(27600) |
| <u>6</u> | 710(2300), 540(7700)  | 452sh(11500), 360(29000), 316sh(23200),<br>216(30400) |

sh shoulder.

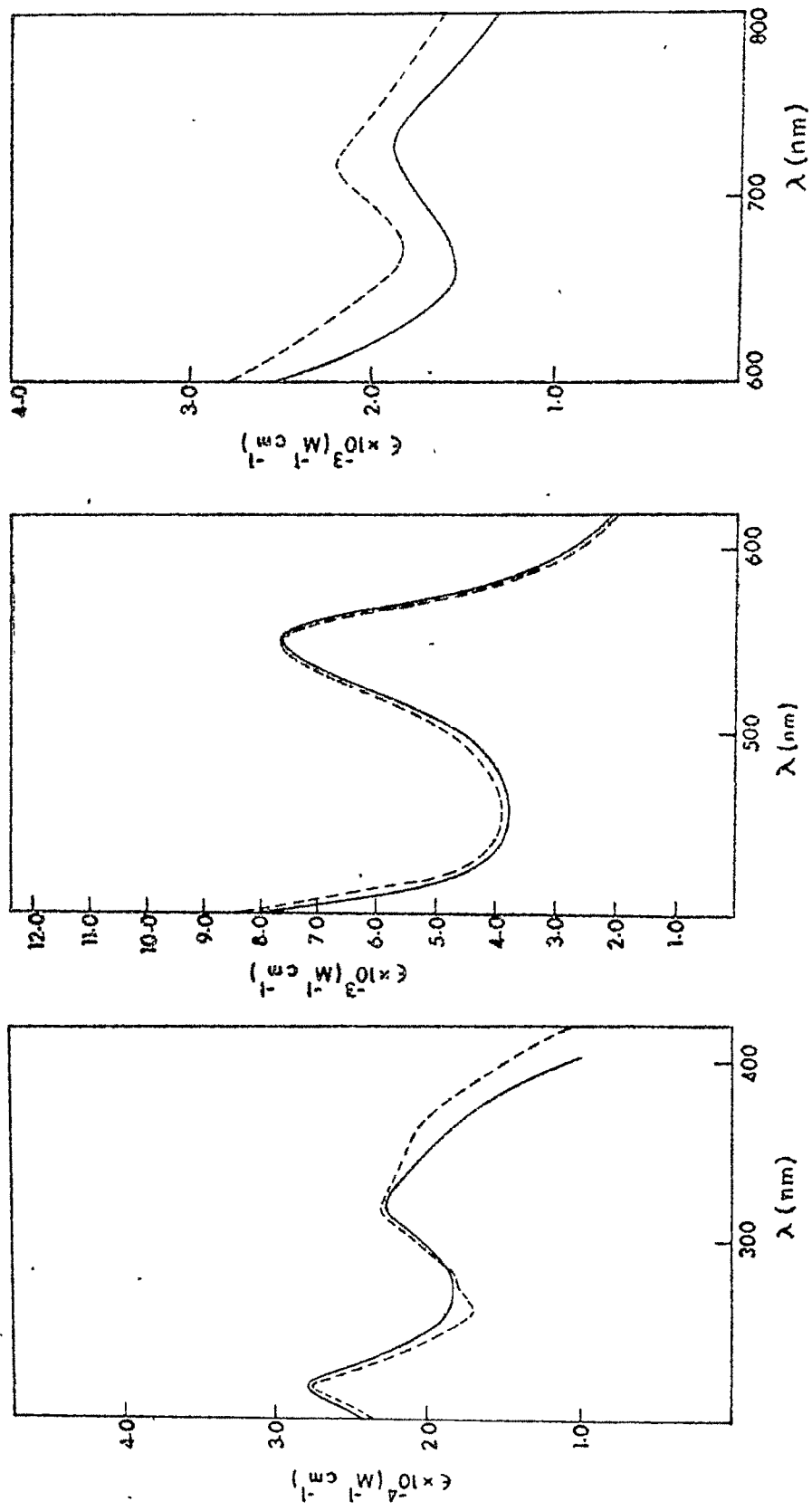


FIG VIII.2 ELECTRONIC SPECTRA OF 2 (—) AND 5 (---) IN  $\text{CH}_3\text{CN}$

Electrochemical Data<sup>a-c</sup> of  $[\text{Ru}(\text{pap})_2\text{F}]\text{ClO}_4 \cdot \text{H}_2\text{O}$  Complexes in Acetonitrile (298K) at Pt Electrode

| Complex  | $v, \text{mVs}^{-1}$ | $E_{\text{pc}}, \text{V}$ | $E_{\text{pa}}, \text{V}$ | $E_{298}^0, \text{V}$ | $\Delta E_{\text{p}}, \text{mV}$ |
|----------|----------------------|---------------------------|---------------------------|-----------------------|----------------------------------|
| <u>1</u> | 20                   | 0.670                     | 0.740                     | 0.705                 | 70                               |
|          | 50                   | 0.670                     | 0.740                     | 0.705                 | 70                               |
|          | 100                  | 0.665                     | 0.745                     | 0.705                 | 80                               |
| <u>2</u> | 20                   | 0.740                     | 0.800                     | 0.770                 | 60                               |
|          | 50                   | 0.740                     | 0.810                     | 0.775                 | 70                               |
|          | 100                  | 0.740                     | 0.820                     | 0.780                 | 80                               |
| <u>3</u> | 50                   | 0.780                     | 0.850                     | 0.815                 | 70                               |
|          | 100                  | 0.780                     | 0.860                     | 0.820                 | 80                               |
| <u>4</u> | 20                   | 0.810                     | 0.870                     | 0.840                 | 60                               |
|          | 50                   | 0.810                     | 0.870                     | 0.840                 | 60                               |
|          | 100                  | 0.810                     | 0.880                     | 0.845                 | 70                               |
|          | 200                  | 0.810                     | 0.890                     | 0.850                 | 80                               |
| <u>5</u> | 50                   | 0.855                     | 0.930                     | 0.893                 | 75                               |
|          | 100                  | 0.855                     | 0.930                     | 0.893                 | 75                               |
| <u>6</u> | 20                   | 0.890                     | 0.960                     | 0.925                 | 70                               |
|          | 50                   | 0.890                     | 0.960                     | 0.925                 | 70                               |

<sup>a</sup> Meaning of units and symbols are the same as in text. <sup>b</sup> Supporting electrolyte, TEAP (0.1M).

<sup>c</sup> 4.56 mg of complex 2 exhaustively oxidized at + 1.2V, Q: calcd. 0.58; found, 0.62; 4.1 mg of complex 5 oxidized at + 1.25V, Q: calcd., 0.48; found, 0.53.

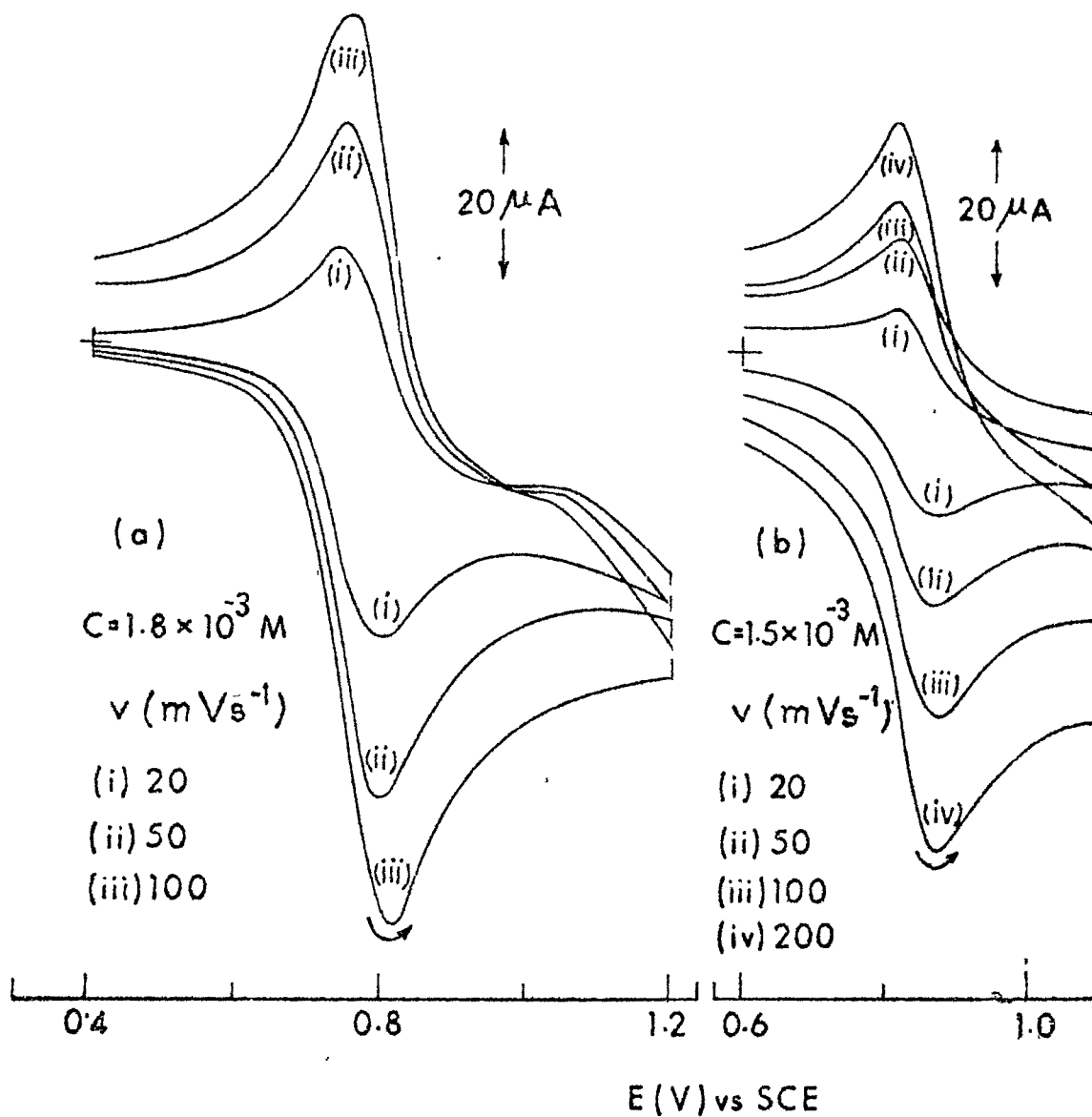
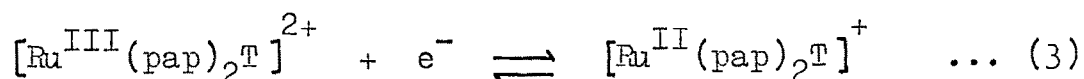


FIG. VIII.3. CVGRAMS OF (a) 2 AND (b) 4 IN  $\text{CH}_3\text{CN}$  AT Pt ELECTRODE

At slow scan rates ( $v < 50 \text{ mVs}^{-1}$ )  $\Delta E_p$  is  $\sim 70 \text{ mV}$ , suggesting the general reversible nature of the electrode reaction (3).



Exhaustive electrolysis (coulometry) of 2 and 5 gave coulomb count (Table VIII.4) corresponding to the transfer of one electron. Isolation of salts from coulometrically oxidized species are under way.

The formal electrode potentials  $E_{298}^0$  (i.e., the average of anodic and cathodic peak potentials) for the couple (3) are given in Table VIII.4.

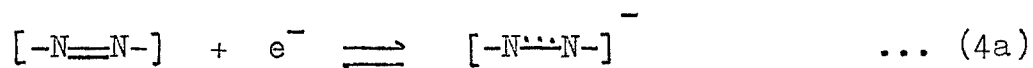
The ruthenium(III)-ruthenium(II) redox potentials of  $[\text{Ru}(\text{pap})_2\text{T}]^+$  (0.71 to 0.93V) (R=Et)(Table VIII.4) are considerably higher than those of other  $[\text{Ru}(\text{bpy})_2(\text{LL}') ]^{n+}$  species (Chapter VII, Table VII.7). The following observations are in order. The  $E_{298}^0$  of  $[\text{Ru}(\text{bpy})_2(\text{pap})]^{2+}$  (1.60V)<sup>1</sup> exceeds that of  $[\text{Ru}(\text{bpy})_3]^{2+}$  (1.29V)<sup>6</sup> by  $\sim 0.3\text{V}$ . Assuming additivity, one may expect the  $E_{298}^0$  of  $[\text{Ru}(\text{pap})_2\text{T}]^+$  to be  $\sim 0.6\text{V}$  larger than that of  $[\text{Ru}(\text{bpy})_2\text{T}]^+$  (0.16 to 0.36V) (R=Et)(Chapter VII, Table VII.7). This is indeed observed.

#### (b) Ligand Reduction

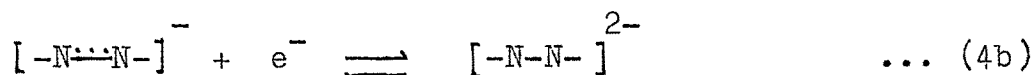
For all complexes (1-6) multiple electrochemical responses (reversible to quasireversible) were observed in the range  $-0.4$  to  $-2.3\text{V}$  vs SCE at platinum or mercury working electrode.

Data taken in acetonitrile solution are collected in Table VIII.5 and Fig. VIII.4.

It is known that the azo group can undergo the following two successive one-electron reductions in aprotic solvents<sup>7-10</sup>



and



In  $[\text{Ru}(\text{pap})_2\text{T}]^+$  species, two azo functions are present one in each pap moiety. Hence, four reductions could, in principle, be observable. In the case of 2, measurements were down to -2.4V using HMDE as the working electrode. Four responses were indeed observed using CV (Fig. VIII.5) and DPV (Fig. VIII.6) (Table VIII.5).

The couples at  $\sim -0.5\text{V}$  (first reduction) and  $\sim -1.0\text{V}$  (second reduction) are assigned to electrode reactions of type (4a) occurring at two different azo functions. Since the two electrons go to two different functions, the potentials are relatively close to each other. The couples at  $\sim -1.9\text{V}$  and  $\sim -2.2\text{V}$  are due to electrode reactions of type (4b). The relatively large potential gap between the (4a) type and (4b) type couples reflects the electrostatic repulsion of two electrons entering into the same azo group.



Table VIII.5

Ligand Reduction Data<sup>a-d</sup> (298K) of  $[\text{Ru}(\text{pap})_2\text{T}]\text{ClO}_4 \cdot \text{H}_2\text{O}$  Complexes  
in Acetonitrile (0.1M in TEAP) Solution

| Complex              | $E_{pc}, V$ | $E_{pa}, V$ | $E_{298}^0 (CV), V$ | $\Delta E_p, mV$ | $E_{298}^0 (DPV)^e, V$ |
|----------------------|-------------|-------------|---------------------|------------------|------------------------|
| <u>1</u>             | -0.53       | -0.47       | -0.50               | 60               |                        |
|                      | -1.09       | -0.99       | -1.04               | 100              |                        |
| <u>2<sup>c</sup></u> | -0.53       | -0.47       | -0.50               | 60               |                        |
|                      | (-0.56)     | (-0.50)     | (-0.53)             | (60)             | (-0.54)                |
|                      | -1.08       | -1.02       | -1.05               | 60               |                        |
|                      | (-1.11)     | (-1.00)     | (-1.06)             | (110)            | (-1.12)                |
|                      | (-1.94)     | (-1.88)     | (-1.91)             | (60)             | (-1.98)                |
|                      | (-2.24)     | (-2.18)     | (-2.21)             | (60)             | (-2.26)                |
| <u>3</u>             | -0.52       | -0.44       | -0.48               | 80               |                        |
|                      | -1.13       | -1.01       | -1.07               | 120              |                        |
| <u>4</u>             | -0.47       | -0.38       | -0.43               | 90               |                        |
|                      | -1.00       | -0.91       | -0.96               | 90               |                        |
| <u>5</u>             | -0.47       | -0.39       | -0.43               | 80               |                        |
|                      | -1.01       | -0.93       | -0.97               | 80               |                        |
| <u>6</u>             | -0.45       | -0.37       | -0.41               | 80               |                        |
|                      | -0.97       | -0.89       | -0.93               | 80               |                        |

<sup>a</sup> Meaning of units and symbols are the same as in text.

<sup>b</sup> Unless otherwise stated the electrode is platinum.

<sup>c</sup> The values given in parentheses are at hanging mercury drop electrode (HMDE). <sup>d</sup> CV: Scan rate =  $50 \text{ mVs}^{-1}$ ; for 2 it is  $100 \text{ mVs}^{-1}$ ; DPV: Scan rate =  $20 \text{ mVs}^{-1}$ ; Modulation Amplitude = 25 mV; Drop time = 0.5 sec. <sup>e</sup> Calculated using eq (13) of Chapter I.

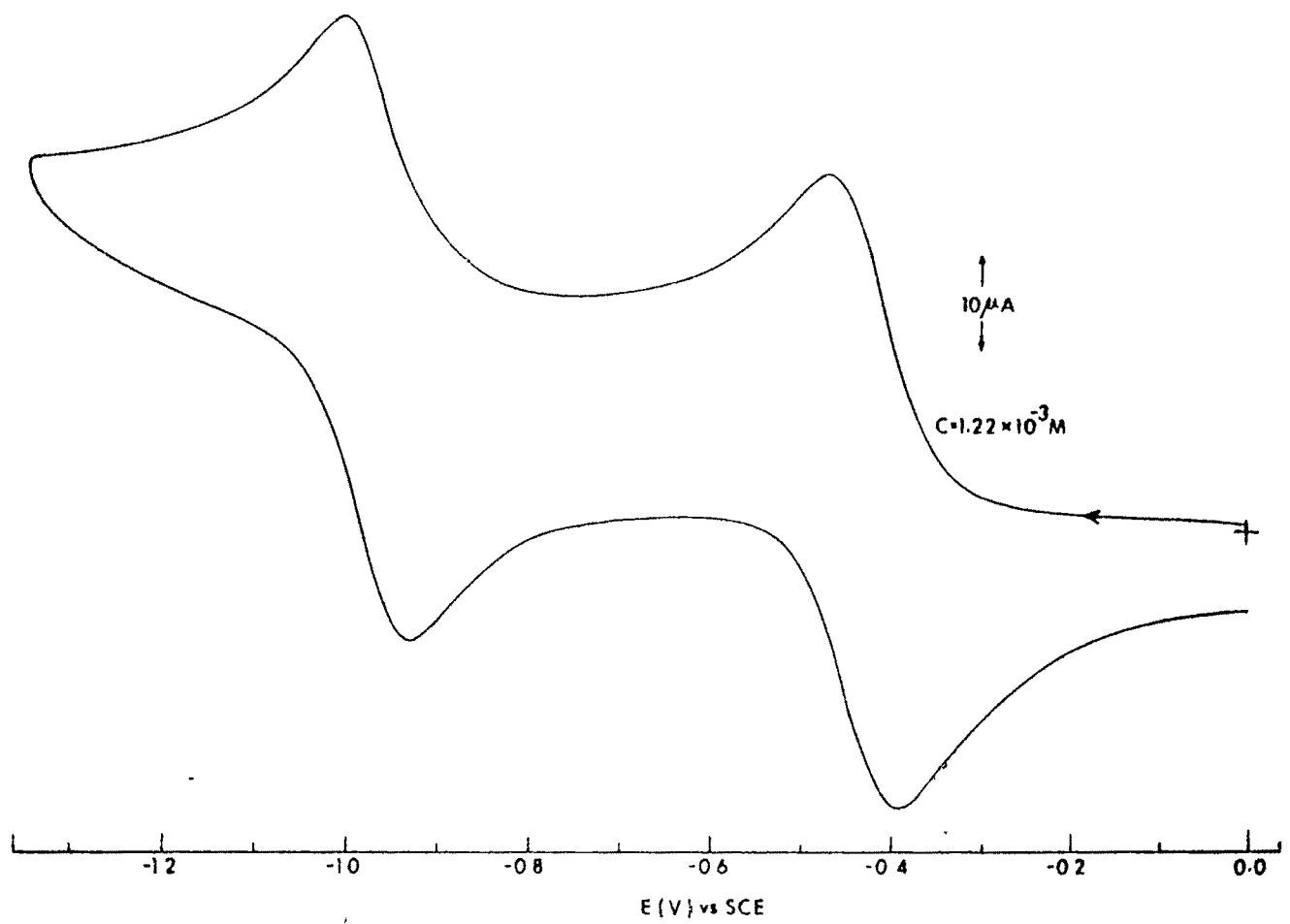


FIG VIII 4 CV RESPONSE OF 5 IN  $\text{CH}_3\text{CN}$  AT Pt ELECTRODE ( $v = 50 \text{ mVs}^{-1}$ )

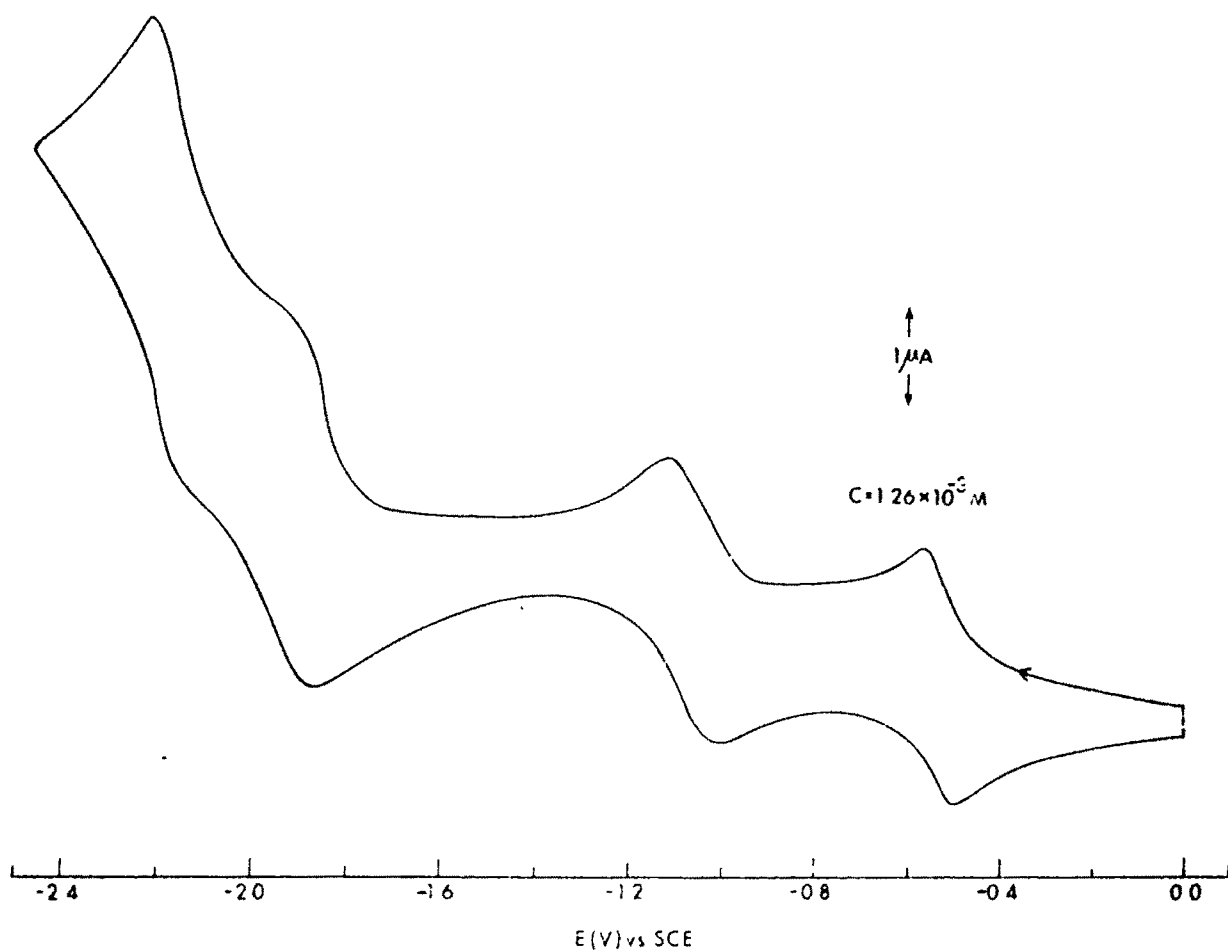


FIG VIII 5 CVGRAM OF 2 IN  $\text{CH}_3\text{CN}$  AT HMDE ( $\nu = 100 \text{ mVs}^{-1}$ )

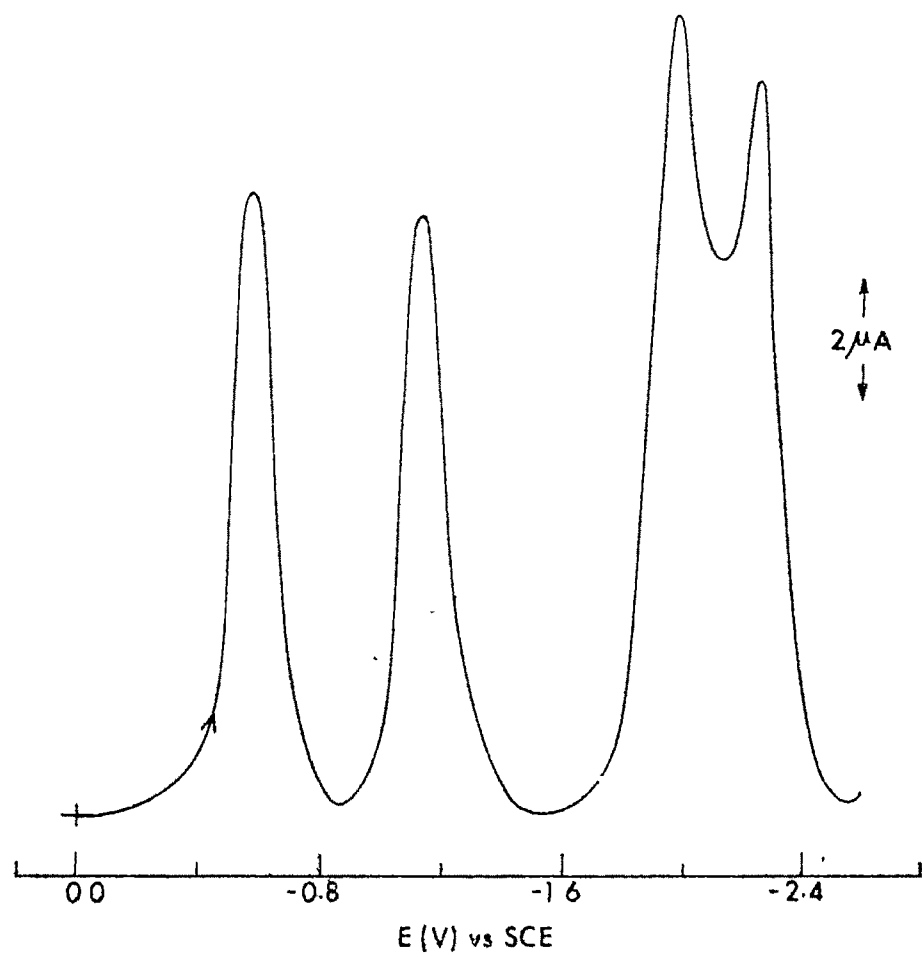


FIG. VIII. 6. DPV GRAM OF 2 IN  $\text{CH}_3\text{CN}$  ( $0.63 \times 10^{-3} \text{ M}$ ) AT HMDE ( $v = 20 \text{ mVs}^{-1}$ )

In the case of other complexes the measurements were limited to  $-1.5\text{V}$  and only two responses were located (Table-VIII.5)(Fig. VIII.4).

The formal potentials of these were found to shift with substituents (X) present at the triazene 1-oxide fragment, showing that interchelate interaction via metal exists. The Hammett  $E_{298}^{\circ} - \sigma$  correlations are fair to good (Fig. VIII.7). The  $\rho$  values are :  $0.09\text{V}$  (couple  $\sim -0.5\text{V}$ ) and  $0.13\text{V}$  (couple  $\sim -1.0\text{V}$ ).

#### E. Linear Free Energy Relationships

In the complexes 1-6, the  $E_{298}^{\circ}$  values of  $\text{Ru}^{\text{III}}/\text{Ru}^{\text{II}}$  couple are sensitive to the substituent X present at the triazene 1-oxide frame (Table VIII.4). When OMe group is replaced by  $\text{NO}_2$ , the  $\text{Ru}^{\text{II}} \rightarrow \text{Ru}^{\text{III}}$  potential is increased by  $220\text{ mV}$  (Table VIII.4).

When X is systematically varied, the relationship (5) holds,

$$\Delta E_{298}^{\circ} = \sigma \rho \quad \dots (5)$$

The symbols have their usual significance as before. The  $\sigma$  values used are given in Chapter II. The  $E_{298}^{\circ} - \sigma$  plot is linear (Fig. VIII.8). The present  $\rho$  value ( $0.19\text{V}$ ) is comparable to the value of  $[\text{Ru}(\text{bpy})_2\text{T}]^+$  species (Chapter VII).

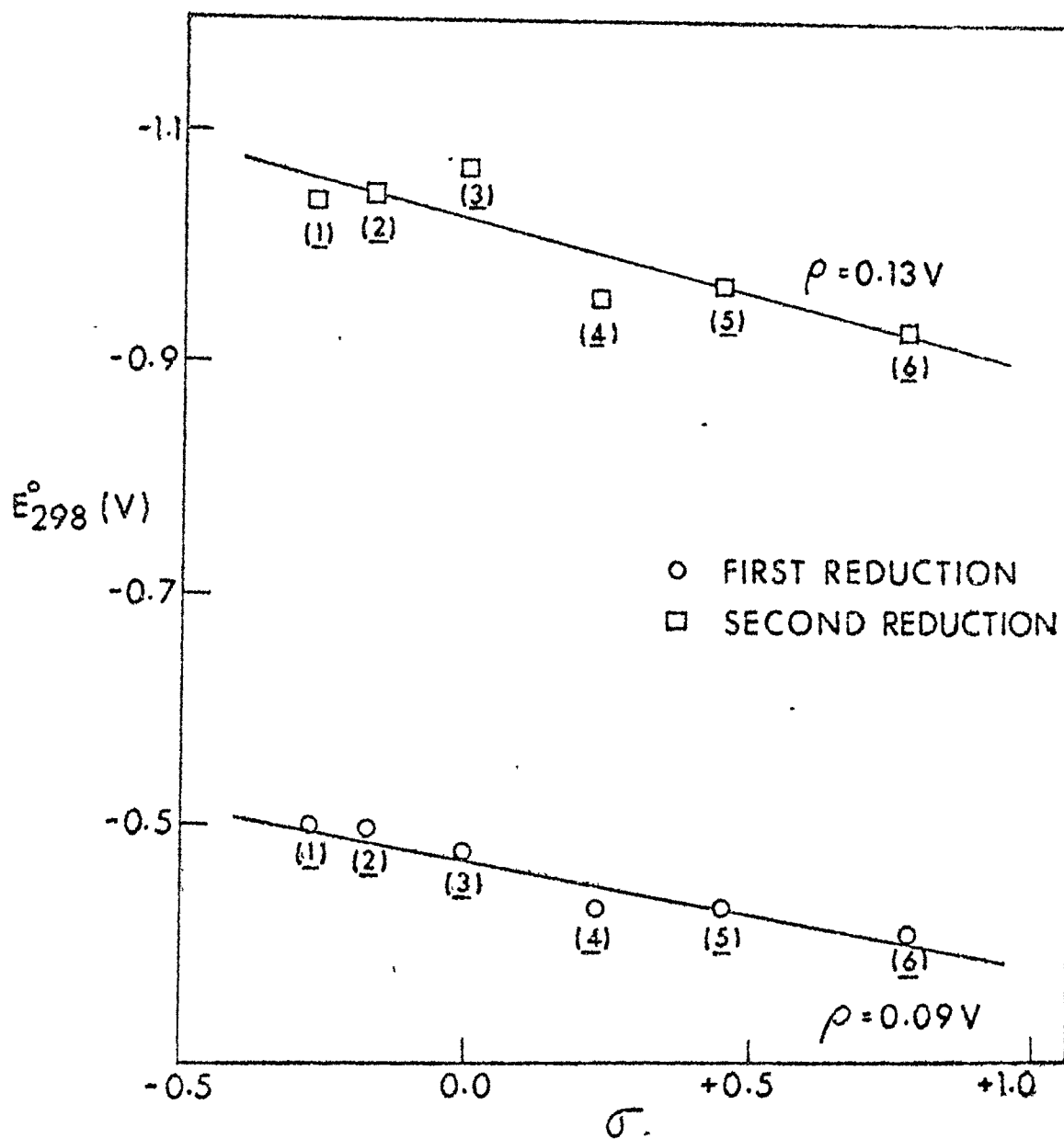


FIG. VIII. 7.  $E_{298}^{\circ}$  (AZO-REDUCTIONS)- $\sigma$  PLOT FOR  
 $[\text{Ru}(\text{pap})_2\text{T}] \text{ClO}_4 \cdot \text{H}_2\text{O}$

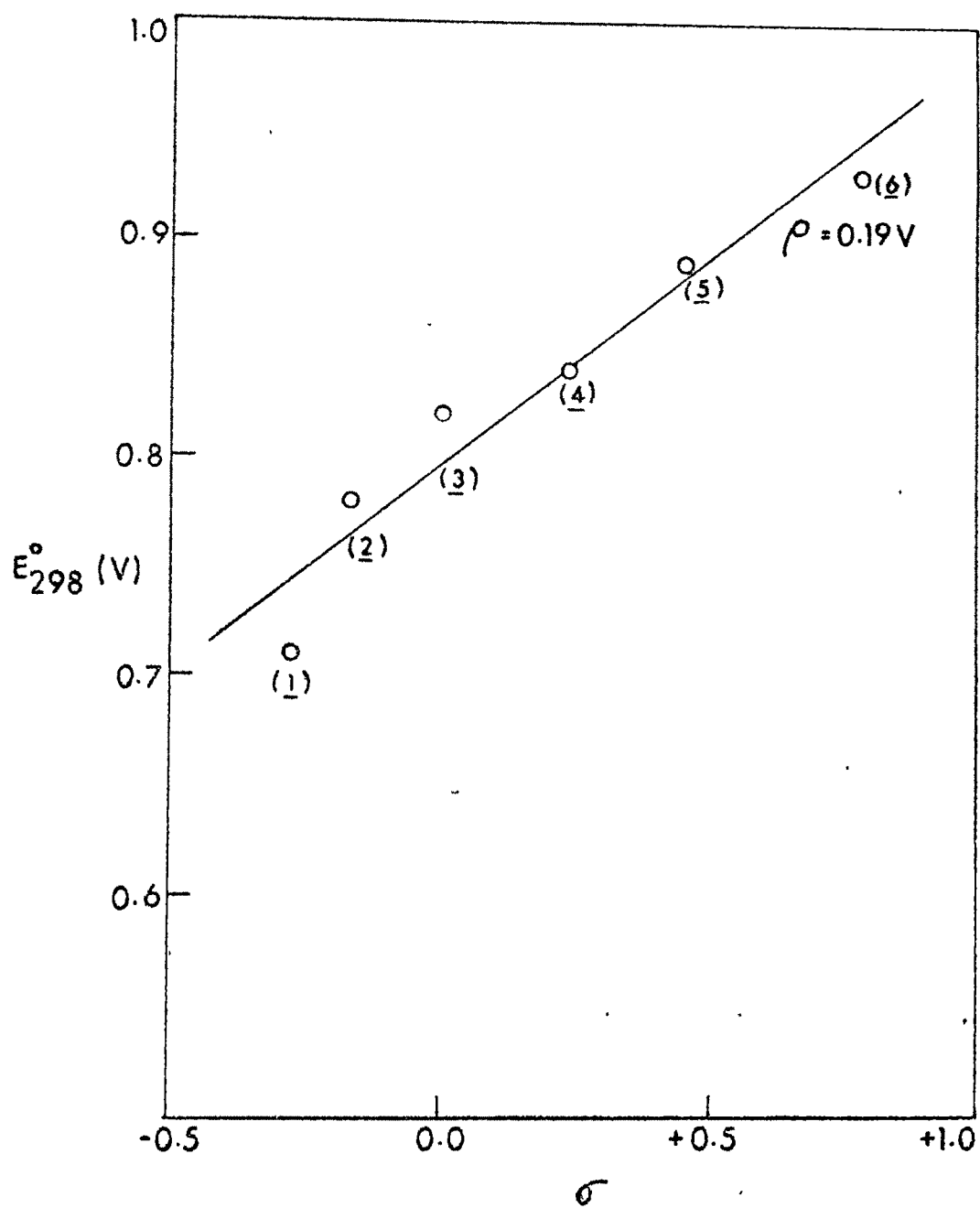


FIG.VIII.8.  $E_{298}^{\circ}$ - $\sigma$  PLOT FOR  $[\text{Ru}(\text{pap})_2 \text{T}] \text{ClO}_4 \cdot \text{H}_2\text{O}$

F. The Oxidized Species  $[\text{Ru}^{\text{III}}(\text{pap})_2\text{T}]^{2+}$

Unlike  $[\text{Ru}^{\text{II}}(\text{bpy})_2\text{T}]^+$  (Chapter VII), the oxidation of the present complexes occurs at relatively high positive potential making the ruthenium(III) species strong oxidant and therefore quite reactive. Bronze coloured  $[\text{Ru}^{\text{III}}(\text{pap})_2\text{T}]^{2+}$ , present in the coulometrically oxidized solution of  $[\text{Ru}(\text{pap})_2\text{T}]^+$  is not particularly stable and is transformed to the original red-violet colour within 0.5h.

The electronic spectral data of fresh solution (coulometrically oxidized) of the complexes 2 and 5 are given in Table VIII.6 and spectra of 5 is displayed in Fig. VIII.9.

In the visible region, three bands at  $\sim 740$  nm,  $\sim 550$  nm and  $\sim 500$  nm are observed. As before ( $[\text{Ru}^{\text{III}}(\text{bpy})_2\text{T}]^+$ ; Chapter VII), the lowest energy band is assigned to  $\pi(\text{T}) \rightarrow t_2(\text{Ru})(\text{LMCT})$  transition. The bands at  $\sim 550$  nm and  $\sim 500$  nm are assigned to  $\pi(\text{pap}) \rightarrow t_2(\text{Ru})(\text{LMCT})$ .

G. Summary of  $\rho$  values in LFER Studies

The  $\rho$  values (only for metal-centered redox reactions) for all systems studied during the present investigation are collected in Table VIII.7.

For six bonds away substituents (X) the values are comparable among all tris species. When number of bonds between



Table VIII.6

Electronic Spectral Data of  $[\text{Ru}(\text{pap})_2\text{T}]^{2+}$  Complexes in Acetonitrile

| Complex         | $\lambda_{\text{nm}} (\epsilon, \text{M}^{-1} \text{cm}^{-1})$ | IMCT bands                           | Other bands              |
|-----------------|--|--------------------------------------|--------------------------|
| $\underline{2}$ |  | 754(4000), 548sh(6900),<br>494(7600) | 362(23900), 316sh(21200) |
| $\underline{5}$ |  | 728(2600), 530(7200),<br>514sh(7000) | 360(24600), 312sh(20600) |

sh shoulder.

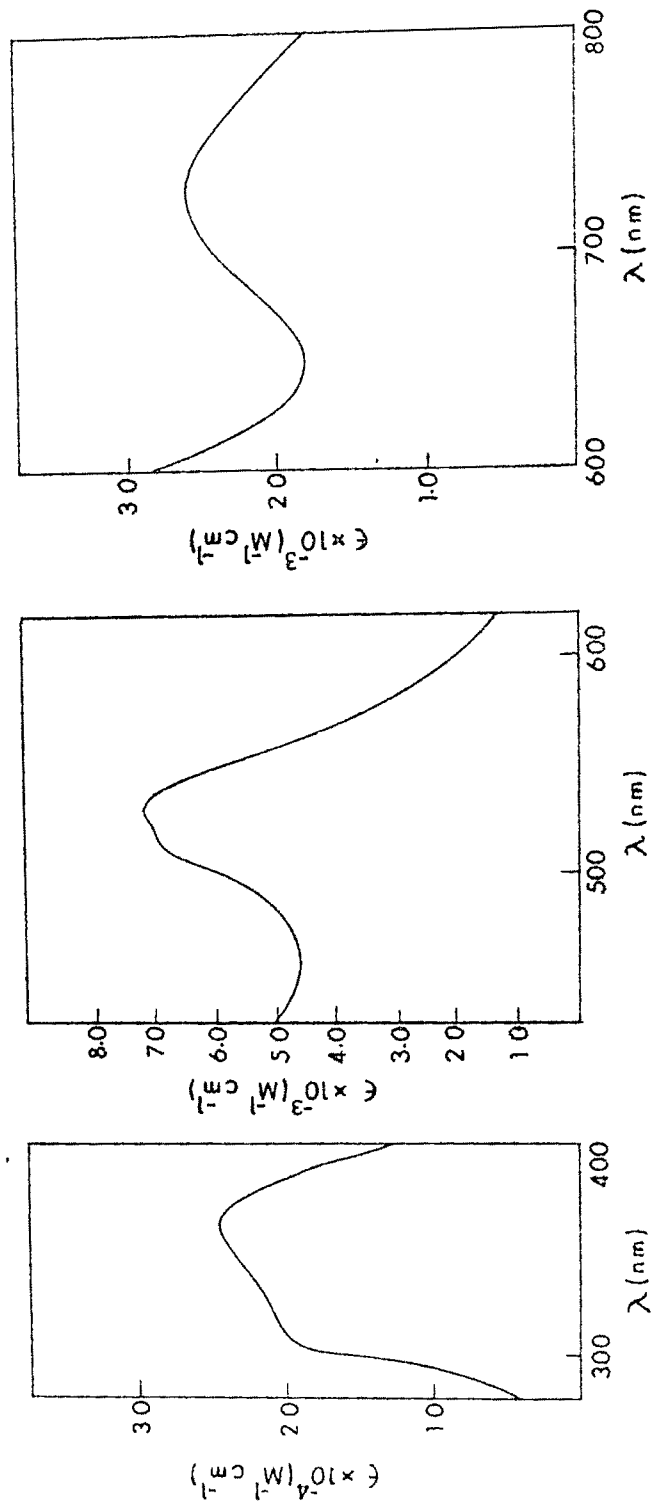


FIG. VIII. 9. ELECTRONIC SPECTRA OF COULOMETRICALLY OXIDIZED S IN CH<sub>3</sub>CN

Comparison of  $\rho$  values

| Species                                      | Nature of substituent | Couple         | $E_{298}^0, V$ | Number of bonds between metal and substituent | $\rho, V$ | Ref.         |
|--|-----------------------|----------------|----------------|---|-----------|--------------|
| 1. $FeT_3$ (R=Et)                            | X                     | Fe(III)/Fe(II) | -0.32 to -0.76 | 6   | 0.16      | Chapter II   |
| 2. $FeT_3$ (R=Ph)                            | X                     | "              | -0.15 to -0.50 | 6   | 0.11      | "            |
| 3. $CoT_3$ (R=Et)                            | X                     | Co(III)/Co(II) | -0.08 to -0.56 | 6   | 0.17      | "            |
| 4. $FeT_3$                                   | Y                     | Fe(III)/Fe(II) | -0.43 to -0.53 | 7   | 0.08      | "            |
| 5. $CuT_2$ (R=Et)                            | X                     | Cu(II)/Cu(I)   | -0.46 to -0.84 | 6   | 0.17      | Chapter III  |
| 6. $CuT_2$ (R=Ph)                            | X                     | "              | -0.37 to -0.66 | 6   | 0.13      | "            |
| 7. $CuT_2$ (R=Et)                            | Z                     | "              | -0.81 to -0.91 | 4   | 0.10      | "            |
| 8. $RuT_3$ (R=Et)                            | X                     | Ru(III)/Ru(II) | -0.69 to -1.20 | 6   | 0.18      | Chapter VI   |
| 9. $RuT_3$ (R=Ph)                            | X                     | "              | -0.66 to -0.83 | 6   | 0.10      | "            |
| 10. $RuT_3$ (R=Et)                           | X                     | Ru(IV)/Ru(III) | +0.24 to 0.60  | 6   | 0.13      | "            |
| 11. $RuT_3$ (R=Ph)                           | X                     | "              | 0.45 to 0.66   | 6   | 0.11      | "            |
| 12. $Ru(bpy)_2^T ClO_4 \cdot H_2O$<br>(R=Et) | X                     | Ru(III)/Ru(II) | 0.16 to 0.36   | 6   | 0.19      | Chapter VII  |
| 13. $Ru(bpy)_2^T ClO_4 \cdot H_2O$<br>(R=Ph) | X                     | "              | 0.25 to 0.44   | 6   | 0.21      | "            |
| 14. $Ru(pap)_2^T ClO_4 \cdot H_2O$<br>(R=Et) | X                     | "              | 0.71 to 0.93   | 6   | 0.19      | Chapter VIII |

metal and substituent increases  $\rho$  values decrease. (Y substituents in  $\text{FeT}_3$  group, Table VIII.6). The values for copper(II) bis complexes are comparable to  $\text{FeT}_3$ ,  $\text{CoT}_3$  and  $\text{RuT}_3$ . The values for  $[\text{Ru}(\text{bpy})_2\text{T}]^+$  and  $[\text{Ru}(\text{pap})_2\text{T}]^+$  group of complexes are almost identical and are slightly higher compared to other systems. In this case the substituent effect might have better transmitted.

#### H. Conclusions

1. The triazene 1-oxides bind with  $\text{C}_2\text{-cis-Ru}(\text{pap})_2^{2+}$  moiety giving rise to shining red-violet complexes of type  $[\text{Ru}(\text{pap})_2\text{T}]\text{ClO}_4 \cdot \text{H}_2\text{O}$ .
2. In the visible region two bands appear at  $\sim 720$  nm and  $\sim 550$  nm. The former relatively low intense band is assigned to  $t_2(\text{Ru}) \longrightarrow \pi^*(\text{T})$  and the latter band to  $t_2(\text{Ru}) \longrightarrow \pi^*(\text{pap})(\text{MLCT})$  transitions.
3. The complexes are electrochemically oxidized at a much higher positive potential compared to the bpy analogue (Chapter VII):  $E_{298}^0$  ( $\text{Ru}(\text{III})/\text{Ru}(\text{II})$ ) = 0.71 to 0.93V vs SCE.
4. The  $E_{298}^0$  shifts systematically with substituent present at the triazene 1-oxide frame. The  $E_{298}^0 - \sigma$  plot is satisfactorily linear. The  $\rho$  parameter thus derived (0.19V) is comparable to the analogous bpy complexes (Table VIII.7).
5. The complexes display ligand reduction responses at the azo function of the pap moiety in the negative side of SCE (-0.4 to -2.3V). The  $E_{298}^0$  values of the first and

second reductions shift with substituents present at the triazene 1-oxide frame. A fair to good linear Hammett correlations are observed. The  $\rho$  values are: 0.09V (first reduction) and 0.13V (second reduction).

6. The coulometrically oxidized species  $[\text{Ru}(\text{pap})_2\text{T}]^{2+}$  exhibit in the visible region, three bands at  $\sim 740$  nm,  $\sim 550$  nm and  $\sim 500$  nm. The lowest energy band is assigned to  $\pi(\text{T}) \longrightarrow t_2(\text{Ru})(\text{LMCT})$  transition. The bands at  $\sim 550$  nm and  $\sim 500$  nm are assigned to  $\pi(\text{pap}) \longrightarrow t_2(\text{Ru})(\text{LMCT})$ .

### VIII.3 EXPERIMENTAL SECTION

#### A. Preparation of Compounds

##### a. Preparation of Ligands

2-phenylazopyridine(pap) was synthesized by condensing 2-aminopyridine with nitrosobenzene according to reported procedure<sup>11</sup> with the modification that chromatographic purification was done on a column of silica gel instead of alumina. On silica gel a better separation of bands was achieved.

The triazene 1-oxides were prepared as described in Chapter II.

##### b. Preparation of Complexes

ttt-Dichlorobis(2-phenylazopyridine)ruthenium(II),  $\text{Ru}(\text{pap})_2\text{Cl}_2$  was synthesized according to reported procedure<sup>1</sup>. It was then converted to the  $\text{C}_2$ -isomer<sup>2</sup> by boiling in xylene.

Bis(2-phenylazopyridine)(triazene 1-oxidato)ruthenium(II)  
perchlorate monohydrate,  $[\text{Ru}(\text{pap})_2\text{T}]\text{ClO}_4 \cdot \text{H}_2\text{O}$  complexes were  
 synthesized following the general procedure.

To a solution of 100 mg of  $\text{C}_2\text{-Ru}(\text{pap})_2\text{Cl}_2$  (0.19 mmol) in 15 ml dry methanol was added 90 mg (0.40 mmol) of  $\text{AgClO}_4$ . The reaction mixture was refluxed for 1h. After cooling the mixture at room temperature it was filtered through G-4 gooch. To the violet coloured disolvento species 50 mg (0.25 mmol) of 1-ethyl 3-p-chloro phenyl triazene 1-oxide and 50 mg  $\text{K}_2\text{CO}_3$  (0.36 mmol) were added and refluxed under nitrogen atmosphere for 2h. Then the reaction mixture was allowed to cool at room temperature. After evaporation of solvent red-violet crystals separated. Washed several times with ice cold water and diethyl ether and dried in vacuo over  $\text{P}_4\text{O}_{10}$ . The yield was ~ 50%.

c. Tetraethylammonium Perchlorate (TEAP)

It was prepared as described in Chapter II.

B. Characterization of Complexes

Complexes were characterized by C,H,N,Cl microanalyses which was done from C.S.I.R.O., Australia. Data are collected in Table VIII.8.

Table VIII.8

## Characterization Data of Complexes

| Serial Number | Formula                     | % C    |       | % H    |       | % N    |       | % Cl   |       |
|---------------|-----------------------------|--------|-------|--------|-------|--------|-------|--------|-------|
|               |                             | Calcd. | Found | Calcd. | Found | Calcd. | Found | Calcd. | Found |
| <u>1</u>      | $C_{31}H_{32}N_9O_7ClRu$    | 47.78  | 47.91 | 4.11   | 3.94  | 16.18  | 16.57 | 4.56   | 4.54  |
| <u>2</u>      | $C_{31}H_{32}N_9O_6ClRu$    | 48.78  | 48.52 | 4.20   | 3.85  | 16.52  | 16.59 | 4.66   | 4.63  |
| <u>3</u>      | $C_{30}H_{30}N_9O_6ClRu$    | 48.09  | 48.53 | 4.01   | 4.00  | 16.83  | 17.01 | 4.74   | 4.76  |
| <u>4</u>      | $C_{30}H_{29}N_9O_6Cl_2Ru$  | 45.97  | 46.02 | 3.70   | 3.72  | 16.09  | 16.10 | 9.07   | 9.12  |
| <u>5</u>      | $C_{33}H_{34}N_9O_8ClRu$    | 48.26  | 48.21 | 4.14   | 4.07  | 15.35  | 15.39 | 4.33   | 4.35  |
| <u>6</u>      | $C_{30}H_{29}N_{10}O_8ClRu$ | 45.36  | 46.42 | 3.65   | 3.48  | 17.64  | 18.05 | 4.47   | 4.52  |

C. Solvent

Electrochemical grade acetonitrile was prepared as described in Chapter II.

D. Physical Measurements

Electrical Conductance, Infrared Spectra, Electronic Spectra, Electrochemical Measurements: Details are in Chapters II-VII.



REFERENCES

1. S. Goswami, A.R. Chakravarty and A. Chakravorty, Inorg. Chem., 20, 2246 (1981); 21, 0000 (1982).
2. R.A. Krause and K. Krause, Inorg. Chem., 19, 2600 (1980).
3. A. Seal and S. Ray, Private Communication.
4. W.J. Greary, Coord. Chem. Rev., 7, 81 (1971).
5. R.L. Dutta and R. Sharma, J. Inorg. Nucl. Chem., 42, 1204 (1981); J.Sci. Ind. Res., 40, 715 (1981).
6. G.M. Brown, T.R. Weaver, F.R. Keene and T.J. Meyer, Inorg. Chem., 15, 190 (1976).
7. A.J. Bard and J.L. Sadler, J. Am. Chem. Soc., 90, 1979 (1968); J.C. Darbrowiak, D.P. Fischer, F.C. McElroy and D.J. Macero, Inorg. Chem., 18, 2304 (1979); K.G. Boto and F.G. Thomas, Aust. J. Chem., 26, 1251 (1973).
8. K.G. Boto and F.G. Thomas, Aust. J. Chem., 24, 975 (1971).
9. G.H. Aylward, J.L. Garnett and J.H. Sharp, Anal. Chem., 39, 457 (1967).
10. P. Bandyopadhyay, P.K. Mascharak and A. Chakravorty, J. Chem. Soc. Dalton Trans., 0000 (1982).
11. N. Campbell, A.W. Henderson and D. Taylor, J. Chem. Soc., 1281 (1953).